



Flow-Mediated Susceptibility and Molecular Response of Cerebral Endothelia to SARS-CoV-2 Infection

Naoki Kaneko, MD, PhD*; Sandro Satta, PhD*; Yutaro Komuro, PhD; Sree Deepthi Muthukrishnan, PhD; Vishesha Kakarla¹, BS; Lea Guo, BS; Jennifer An, BS; Fanny Elahi, MD, PhD; Harley I. Kornblum, MD, PhD; David S. Liebeskind, MD; Tzung Hsiai, MD, PhD; Jason D. Hinman¹, MD, PhD

BACKGROUND AND PURPOSE: Severe acute respiratory syndrome coronavirus-2 (SARS-CoV-2) infection is associated with an increased rate of cerebrovascular events including ischemic stroke and intracerebral hemorrhage. The mechanisms underlying cerebral endothelial susceptibility and response to SARS-CoV-2 are unknown yet critical to understanding the association of SARS-CoV-2 infection with cerebrovascular events.

METHODS: Endothelial cells were isolated from human brain and analyzed by RNA sequencing. Human umbilical vein and human brain microvascular cells were used in both monolayer culture and endothelialized within a 3-dimensional printed vascular model of the middle cerebral artery. Gene expression levels were measured by quantitative polymerase chain reaction and direct RNA hybridization. Recombinant SARS-CoV-2 S protein and S protein-containing liposomes were used to measure endothelial binding by immunocytochemistry.

RESULTS: *ACE2* (angiotensin-converting enzyme-2) mRNA levels were low in human brain and monolayer endothelial cell culture. Within the 3-dimensional printed vascular model, *ACE2* gene expression and protein levels were progressively increased by vessel size and flow rates. SARS-CoV-2 S protein-containing liposomes were detected in human umbilical vein endothelial cells and human brain microvascular endothelial cells in 3-dimensional middle cerebral artery models but not in monolayer culture consistent with flow dependency of *ACE2* expression. Binding of SARS-CoV-2 S protein triggered 83 unique genes in human brain endothelial cells including upregulation of complement component C3.

CONCLUSIONS: Brain endothelial cells are susceptible to direct SARS-CoV-2 infection through flow-dependent expression of *ACE2*. Viral S protein binding triggers a unique gene expression profile in brain endothelia that may explain the association of SARS-CoV-2 infection with cerebrovascular events.

GRAPHIC ABSTRACT: An online [graphic abstract](#) is available for this article.

Key Words: cerebrovascular circulation ■ endothelial cells ■ endothelium, vascular ■ models, theoretical ■ viruses

Infection with severe acute respiratory syndrome coronavirus-2 (SARS-CoV-2) infection is associated with an increased rate of cerebrovascular events including ischemic stroke and intracerebral hemorrhage.^{1–3} Comparisons of ischemic rates in SARS-CoV-2-infected

individuals with historical averages of ischemic stroke rates combine with case series of atypical stroke patients to support an estimated 7-fold increase of stroke in SARS-CoV-2 infection.^{4,5} The mechanisms underlying this cerebrovascular risk are unknown. With infection initiated

Correspondence to: Jason D. Hinman, MD, PhD, Department of Neurology, David Geffen School of Medicine, University of California Los Angeles, Neuroscience Research Bldg, Room 415, 635 Charles E Young Dr S, Los Angeles, CA 90095. Email jhinman@mednetucla.edu

*Drs Kaneko and Satta contributed equally.

The Data Supplement is available with this article at <https://www.ahajournals.org/doi/suppl/10.1161/STROKEAHA.120.032764>.

For Sources of Funding and Disclosures, see page 269.

© 2020 American Heart Association, Inc.

Stroke is available at www.ahajournals.org/journal/str

Nonstandard Abbreviations and Acronyms

3D	3 dimensional
ACE2	angiotensin-converting enzyme-2
hACE2	human angiotensin-converting enzyme-2
HBMEC	human brain microvascular endothelial cell
HUVEC	human umbilical vein endothelial cell
MCA	middle cerebral artery
NF-κB	nuclear factor-kappa B
SARS-CoV-2	severe acute respiratory syndrome coronavirus-2
TMPRSS2	transmembrane protease, serine 2

in the nasopharynx and lung, widespread inflammation activated by this novel coronavirus may trigger a systemic prothrombotic state and circulating cytokines may act on blood-brain barrier permeability,⁶ thereby increasing the risk of both ischemic and hemorrhagic events. While these pathophysiologic mechanisms fit broadly with our understanding of cerebrovascular injury, direct infection of the brain endothelia by SARS-CoV-2 may trigger localized phenomena including thrombosis and cellular permeability. However, the factors that could mediate tropism of SARS-CoV-2 for the cerebral endothelia may help to identify individuals at high risk for cerebrovascular complications associated with SARS-CoV-2 and lessen the burden of stroke associated with this global pandemic.

See related article, p 271

In the lung, the cellular tropism of SARS-CoV-2 is mediated by viral S-protein binding to the hACE2 (human angiotensin-converting enzyme-2), followed by S-protein cleavage by the TMPRSS2 (transmembrane protease, serine 2), allowing viral entry.⁷ ACE2 (angiotensin-converting enzyme-2) expression is reported in both murine cerebral endothelia and pericytes,^{8–10} but there are important molecular differences in murine and hACE2 that limit the value of this observation. ACE2 expression has been reported in human brain, and SARS-CoV-2 RNA can be detected in postmortem brain specimens.¹¹ However, the primary data supporting ACE2 expression and SARS-CoV-2 susceptibility by the cerebral endothelia remain limited. Similarly, the important viral entry cofactor TMPRSS2 is generally absent from human brain,¹⁰ making the true mechanisms of viral susceptibility unknown.

Here, we utilized a novel 3-dimensional (3D) printed endothelialized model system to identify the factors that modulate human cerebrovascular expression of ACE2, how these factors drive susceptibility of brain endothelium to SARS-CoV-2 infection, and the effect of

S-protein binding to the cerebral vasculature. We compared expression of ACE2 and TMPRSS2 in human brain microvascular cells with that of human umbilical vein endothelial cells (HUVECs) under conditions of shear stress in a 3D-printed model of the human middle cerebral artery (MCA). We tested the hypothesis that viral S-protein binding to brain microvascular cells is dependent not only on molecular interaction with ACE2 but also requires a flow-mediated stimulus. We further sought to identify the brain-specific effect on endothelial cell gene expression triggered by viral S-protein binding.

METHODS

The authors declare that all supporting data are available within the article and its [Data Supplement](#).

Patient Samples

We obtained fresh human brain tissue samples from children and adolescents (5–19 years of age) undergoing brain surgeries (temporal or frontal lobe craniotomy) under an approved University of California, Los Angeles Institutional Review Board protocol. The resected tissue consisted of small sections of healthy cortex or white matter and was considered normal according to magnetic resonance imaging and electroencephalogram studies. Samples were collected immediately following surgery.

Magnetic-Activated Cell Sorting for Cell Type Enrichment

We performed magnetic-activated cell sorting using anti-CD31 Dynabeads (Thermo Fisher Scientific) according to manufacturer's protocol to enrich for normal vascular endothelial cells. Three hundred to 700 mg of unsorted portions of normal brain white matter was used as controls. RNA extraction was performed immediately followed by enzymatic dissociation or cell type isolation using Qiagen RNeasy Microkit. Total RNA integrity was examined using the Agilent Bioanalyzer 2000 (Agilent, Santa Clara, CA) and quantified with NanoDrop (Thermo-Fisher, Waltham, MA).

RNA Sequencing and Analysis

One hundred nanograms of cDNA was used for library preparation using Ovation Ultralow Library Systems. All samples were multiplexed into a single pool and sequenced with 50 bp paired end to get ≈ 45 million reads per sample using Illumina HiSeq 2000 sequencer (Illumina, San Diego, CA). Quality control and alignment to the *Homo sapiens* (Hg38) refSeq and gene annotation was performed using STAR. Total counts of read fragments aligned to candidate gene regions were derived using HTSeq program with Human Hg38 as a reference and used as a basis for the quantification of gene expression. Fragments per kilobase per million values were reported as measure of relative expression units.

Modeling

A human-specific intracranial artery stenosis model was created by modifying a prior method to build a brain aneurysm model.^{12,13} Digital Imaging and Communication in Medicine data acquired from computed tomography angiography were

exported, and the 3D vessel image was converted to a stereolithography format (.stl). The wall shear stress distribution, streamlines, and flow velocity were calculated and visualized for the model. Patient-specific vascular molds were fabricated using a Mojo 3D printer (Stratasys, Eden Prairie, MN). The vascular molds made of acrylonitrile butadiene styrene were soaked in acrylonitrile butadiene styrene solvent and chemically smoothed to remove the stair-like layers of the printed objects.¹³ After drying, degassed polydimethylsiloxanes were coated and cured on the cast and hollow stenosis models acquired by removing the mold.

Cell Culture, Endothelialization, and Perfusion Culture

Cell culture: HUVECs and human brain microvascular endothelial cells (HBMECs) were cultured in endothelial cell growth medium 2 (PromoCell) and Complete Classic Medium With Serum and CultureBoost (Cell Systems), respectively, with gentamicin/amphotericin in a CO₂ incubator at 37 °C, and used between passages 6 and 10. To enhance cell adhesion to silicone, silicone tubing and created vascular models were soaked in 10% (3-aminopropyl) trimethoxysilane in 100% ethanol overnight for hydrophilization and in 0.1 mmol/L sulfosuccinimidyl-6-(4'-azido-2'-nitrophenylamino)-hexanoate (sulfo-SANPAH) in water with the aid of UV activation (10 minutes×2 treatments; 365 nm, 36 W, at a distance of 5 cm) for cross-linking.¹³ The models were washed with PBS and coated with fibronectin in PBS at 40 µg/mL. The tubing and vascular models were again washed with PBS and then exposed to UV light for sterilization before cell seeding. HUVECs or HBMECs were attached on the tubing and vascular models using a 3D rotating machine with 2 axes for 48 hours. The tubing or vessel models with endothelial lining were connected to silicone tubes and a perfusion pump, and then culture medium with the viscosity similar to human blood (3.9 cP by dextran) was perfused for 24 hours in a CO₂ incubator.

Quantitative Polymerase Chain Reaction

Triplicate samples of endothelial cell RNA were extracted using Qiagen RNeasy plus micro kit and reverse transcribed to cDNA using SuperScript VILO cDNA Synthesis Kit. Quantitative polymerase chain reaction (qPCR) performed using TaqMan Gene Expression Assays (hACE2, No. 4331182; TMPRSS2, No. 4331182; GAPDH, No. 4453320) and relative expression determined using $\Delta\Delta C_t$ method and results compared by 2-way ANOVA ($P<0.05$).

Liposome Spike S1 Preparation

Rhodamine-containing liposomes (Encapsula Nanoscience) prepared with Immunosome-Biotinyl Cap were coupled to SARS-CoV-2 S1 protein, His, Avitag (ACROBiosystems; No. S1N-C82E8), in a 1:2 ratio and excess S1 protein dialyzed out from the liposome preparation. Control liposome preparations were prepared identically in the absence of SARS-CoV-2 S1 protein. Binding of S-protein liposomes to ACE2 was verified by modified ELISA and in ACE2-transfected human embryonic kidney 293 cells. Liposome preparations were diluted to 1:500 before use, added to cultures or perfusion culture media for 24 hours. Additional details are available in the [Data Supplement](#).

Immunocytochemistry

Endothelial cells were rinsed with PBS, fixed with 2% paraformaldehyde, and multistained with target proteins and 4',6-diamidino-2-phenylindole (nucleus). To observe the ECs on the curved polydimethylsiloxane surface, z stacks were taken every 10 µm to ~800 µm thickness and 2-dimensional maximum intensity projection images were rendered. Mean levels of ACE2 immunostaining in a 1×1-mm field of view ($n=2$) were measured and normalized to phalloidin signal.

Nanostring nCounter Assay

Monolayer cultures of HBMECs and HUVECs were treated with 5 µg/mL of recombinant SARS-CoV-2 Spike (Active Trimer) His Protein (R&D Systems; No. 10549-CV) for 24 hours. Cells were lysed, RNA collected as above, and 100 ng of total RNA was hybridized with probes and run on the nCounter preparation station for removal of excess probes per manufacturer protocol. The number of the target mRNA transcripts was directly counted by digital analyzer. The data were normalized to the geometric means of spiked-in positive controls and spiked-in negative controls and the housekeeping genes. The nSolver software from NanoString was used to normalize count numbers by geometric mean and calculate the fold change and statistical significance, with $P<0.05$ considered significant. Data were visualized using R.

RESULTS

While ACE2 expression has been reported in the human brain, the cell-specific expression pattern of ACE2 is unknown. We isolated CD31+ human endothelial cells from normal brain tissue resected during surgery and performed RNA sequencing ($n=2$). ACE2 levels were below the threshold of detection in both isolated endothelial cells and whole brain white matter indicating low transcriptional expression (Figure 1A). Similarly, recognized SARS-CoV-2 viral entry cofactor, TMPRSS2, demonstrated extremely low transcript detection in isolated CD31+ endothelial cells. Other SARS-CoV-2 viral entry cofactors including PLG (plasminogen) and furin were differentially detected with furin robustly expressed in CD31+ isolated endothelial cells. Existing databases of cultured endothelial cell gene expression demonstrate low levels of ACE2.¹⁴

To determine the effect of vessel size and flow on ACE2 expression, we created a series of 3D vessel models of varying diameter (2–4 mm), endothelialized the luminal surface with HUVECs, and subjected these to 24 hours of perfusion culture (3.9 cP/15 dynes/cm²). Compared with monolayer HUVECs, vessel size drove a significant increase in ACE2 gene expression ($P<0.0001$, $F=55.79$, 1-way ANOVA; Figure 1B). Shear stress in addition to 3D rotational culture further increased ACE2 mRNA levels. To identify the differential effect of shear stress on ACE2 expression, we used a 4-mm vessel endothelialized with HUVECs or HBMECs and subjected these models to normal (15 dynes/cm²) and high (22.5 dynes/cm²) shear stress for 24 hours. Compared with

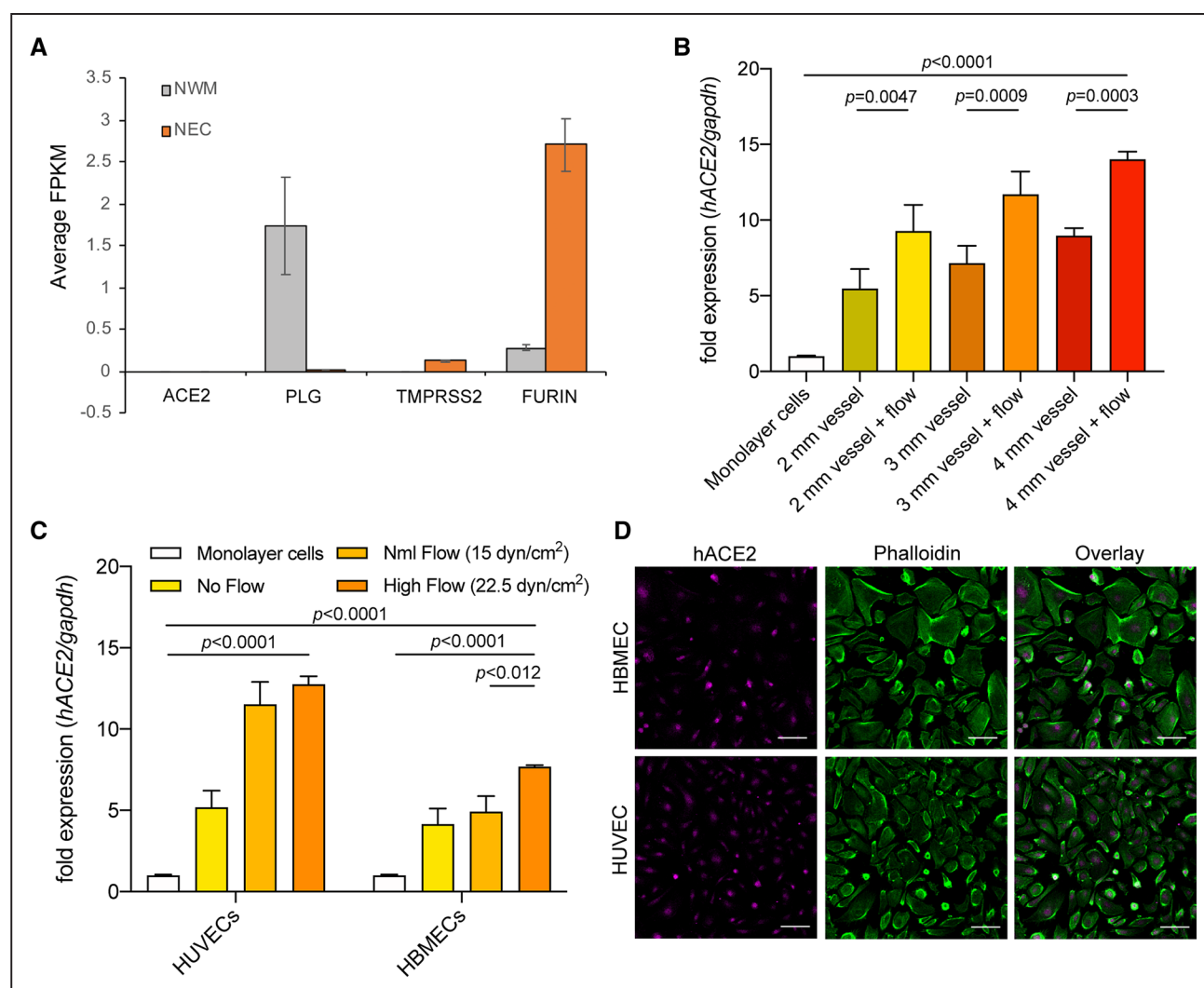


Figure 1. Flow-dependent ACE2 (angiotensin-converting enzyme-2) expression in cerebral endothelial cells.

Average fragments per kilobase per million (FPKM) of gene expression derived from RNA sequencing of normal white matter (NWM; gray) and normal CD31+ endothelial cells (NEC; orange; $n=2$; **A**). Fold expression by quantitative polymerase chain reaction (qPCR) for hACE2 (human ACE2) relative to GAPDH in human umbilical vein endothelial cells (HUVECs) by vessel size and shear stress (15 dynes/cm²; $P<0.0001$ by ANOVA; **B**). Fold expression levels of HUVECs and human brain microvascular endothelial cells (HBMECs) low shear stress vs high shear stress perfusion culture ($P<0.0001$ by 2-way ANOVA; adjusted P provided Tukey post hoc; **C**). Immunocytochemistry for ACE2 in monolayer HBMECs and HUVECs (**D**). Error bars represent SD. Scale bars=100 μ m. PLG indicates plasminogen; and TMPRSS2, transmembrane protease, serine 2.

monolayer cells, shear stress induced *ACE2* gene expression in both HUVECs and HBMECs ($P<0.0001$, $F=153.6$, 2-way ANOVA; Figure 1C). The application of any shear stress triggered *ACE2* expression in HUVECS (adjusted $P<0.0001$), while in HBMECs, the effect of higher shear stress significantly increased *ACE2* expression (adjusted $P=0.012$). Both monolayer HUVECs and HBMECs demonstrated low levels of ACE2 protein expression in cytoplasmic and perinuclear space by immunocytochemistry (Figure 1D). As in the 3D model system, stimulation of monolayer HUVECs and HBMECs with horizontal shear stress increased ACE2 protein expression by Western blot (Figure I in the Data Supplement). Consistent with human brain RNA sequencing, expression of TMPRSS2 could not

be reliably detected at the RNA or protein level in HBMECs across multiple experiments.

Based on the observation that ACE2 expression is triggered by vessel structure and shear stress, we used a computed tomography angiography image of a partially stenosed MCA to 3D print a vessel replica and create a silicone model with the luminal surface lined with HBMECs (Figure 2A). Immunocytochemistry for ACE2 was performed in proximal, stenotic, and distal segments of the MCA model corresponding to regions of normal (≈ 15 dynes/cm²), high (≈ 30 dynes/cm²), and low (<4 dynes/cm²) wall shear stress determined by computational fluid dynamics (Figure 2B). Normalized levels of ACE2 protein expression were determined and found to be significantly increased in the 3D model compared

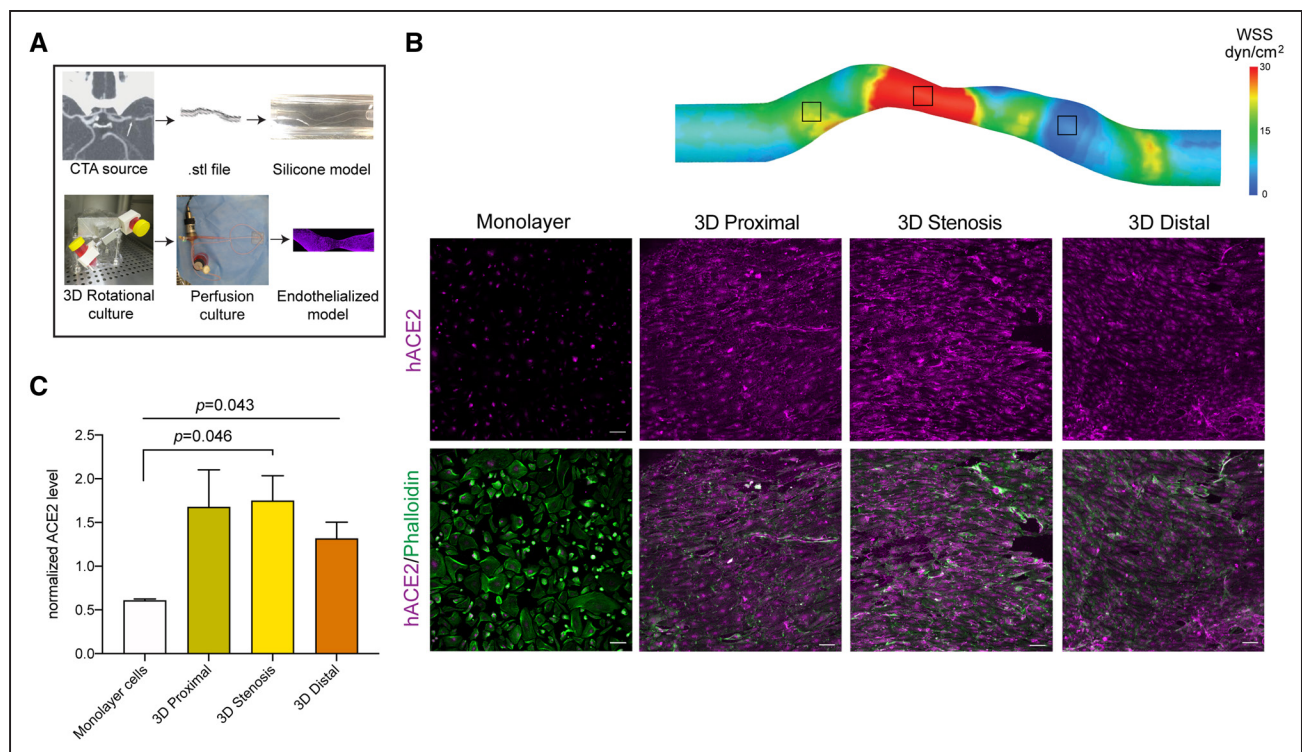


Figure 2. Regional variation in ACE2 (angiotensin-converting enzyme-2) levels using a 3-dimensional (3D) printed middle cerebral artery (MCA) model.

Workflow to generate 3D-printed MCA stenosis model (A). Representative immunocytochemistry for ACE2 in monolayer human brain microvascular endothelial cells, as well as proximal, stenotic, and distal segments of a human brain microvascular endothelialized middle cerebral artery 3D model with computational fluid dynamic modeling of wall shear stress (WSS) across the stenotic model (B). Normalized ACE2 levels (ACE2/phalloidin ratio) in monolayer and segments of MCA 3D model ($P=0.043$ by 1-way ANOVA; adjusted $P=0.046$ by Tukey post hoc comparison of 2-dimensional vs 3D culture; C). Scale bars=100 μm . CTA indicates computed tomography angiography; hACE2, human angiotensin-converting enzyme-2; and .stl, stereolithography format.

with monolayer cells ($P=0.043$, $F=7.27$, 1-way ANOVA). ACE2 expression levels within the stenotic portion of the MCA model were notably higher when compared with monolayer cells (adjusted $P=0.046$; Figure 2C).

The spike protein (S protein) of SARS-CoV-2 binds directly to ACE2 and mediates viral attachment and cellular entry. To determine cerebral endothelial susceptibility to SARS-CoV-2 infection, we prepared S protein-coated liposomes containing fluorescent rhodamine measuring ≈ 100 nm in size (Figures II and III in the Data Supplement). S-protein liposomes bind to hACE2 and can be detected by rhodamine liposome signal in an ACE2 ELISA (Figure 3A). Control and S-protein liposomes were added to monolayer cultures of HUVECs and HBMECs. We observed no measurable cellular detection of S-protein liposomes in either cell type (Figure 3B). Forty-eight hours after endothelialization, we exposed 3D MCA models to 24 hours of flow culture with control and S-protein liposome. Primarily within the stenotic portion of the 3D MCA model, S-protein liposomes were found bound to HBMECs while flow culture with control liposomes were not detected (Figure 3C).

To determine the brain endothelial-specific response of S-protein binding, we used a direct RNA hybridization

assay measuring mRNA expression levels of prespecified 785 host response genes involved in pathways of homeostasis, adaptive immune response, host susceptibility, and interferon response. HBMEC exposure to recombinant S-protein trimer for 24 hours resulted in differential expression of 24 genes (14 upregulated and 10 downregulated; Figure 4A), while the response to recombinant S protein in HUVECs was less robust (17 genes: 4 upregulated and 13 downregulated; Data Supplement). After normalizing across cell types, a distinct brain endothelial-specific gene expression profile was identified containing 80 genes (12 upregulated and 68 downregulated; Figure 4B). Selected genes (*C3* and *CTSW*) differentially expressed in HBMECs were confirmed as upregulated after both S-protein and liposome exposure by qPCR (Figure IV in the Data Supplement). The key upregulated genes by human brain endothelial cells and their association with SARS-CoV-2 infection are presented in the Table.^{15–19}

DISCUSSION

This study establishes 2 critical observations about the potential relationship between SARS-CoV-2 and

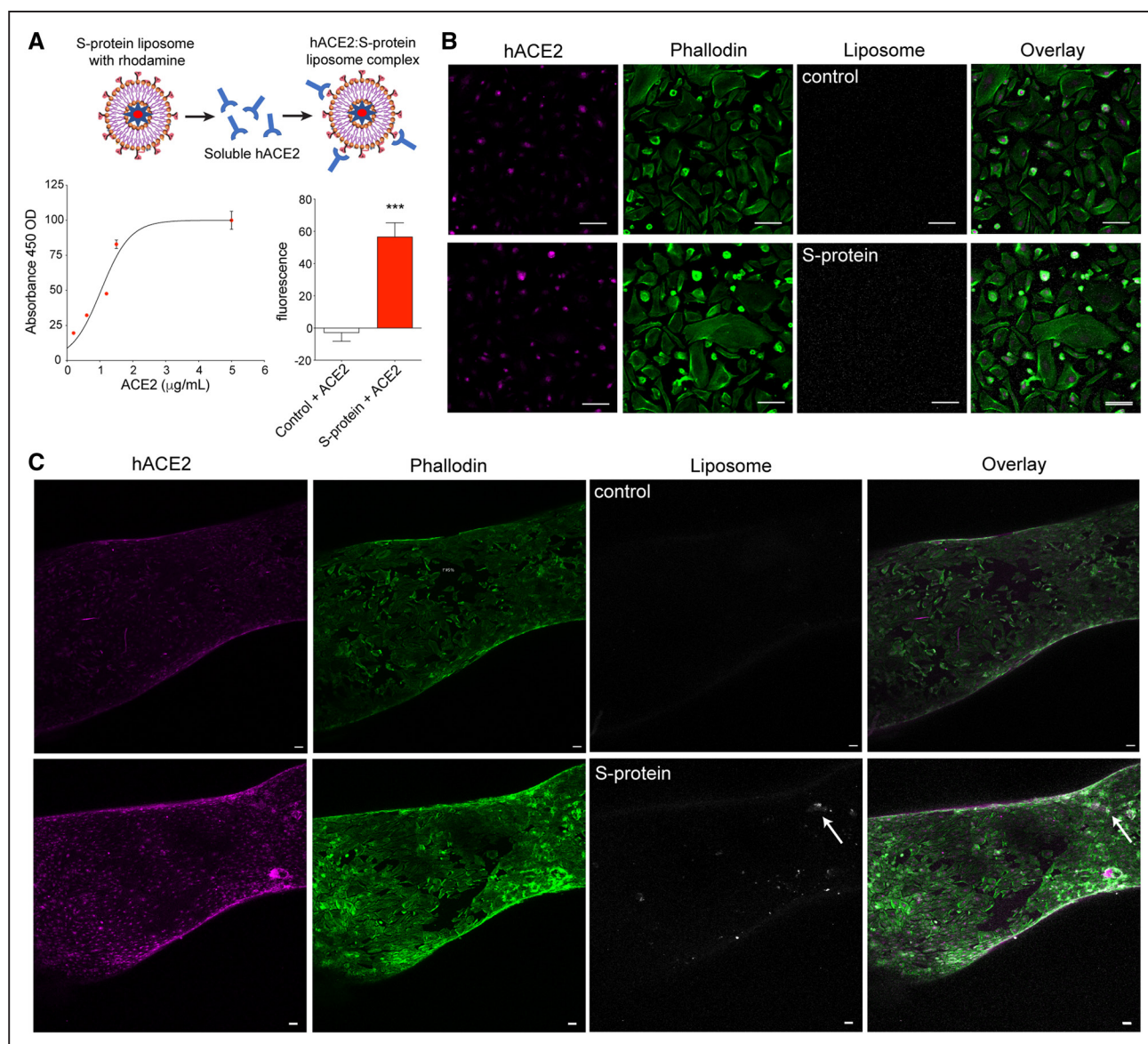


Figure 3. Flow-dependent susceptibility of brain endothelia to severe acute respiratory syndrome coronavirus-2 (SARS-CoV-2) spike protein liposomes.

Liposomes coated with S protein were created as described, incubated with soluble hACE2 (human ACE2 [angiotensin-converting enzyme-2]; 0–5 μg) and S-protein:ACE2 binding detected by ACE2:S-protein sandwich ELISA (left) and intrinsic rhodamine signal (right; **A**). Monolayer human brain microvascular endothelial cells (HBMECs) were exposed to control (top) or S-protein-coated liposomes (bottom; 1:100) for 24 h followed by immunocytochemistry for hACE2 (purple), phalloidin (green), and liposome bound rhodamine (white; **B**). Maximum intensity projection of 3D middle cerebral artery stenosis model endothelialized with HBMECs after 24-h exposure to control (top) or S-protein-coated liposomes (bottom; 1:500; 0.2 μg) during perfusion culture. Bound S-protein liposomes were detected within multiple luminal HBMECs (arrow; **C**). Scale bars=100 μm.

cerebrovascular susceptibility to infection and the brain endothelia-specific response triggered by infection. First, we show that normal *ACE2* gene expression by endothelial cells in human brain is low. In a related fashion, we show that *ACE2* expression is increased by shear stress and that this flow-mediated increase in *ACE2* facilitates susceptibility to SARS-CoV-2 spike protein binding to brain endothelia. Second, we identified a unique gene expression profile within brain endothelia in response to spike protein binding. While prior work has sought to use gene and protein expression levels of *ACE2* in

mouse and human vascular cell types as a surrogate for viral susceptibility, they have not utilized a dynamic flow-dependent model to directly demonstrate viral-endothelial interactions, which we achieved using a novel S protein-coated liposome. With a multiplicity of cerebrovascular pathologies associated with severe SARS-CoV-2 infection including ischemic stroke affecting large and small caliber vessels, microhemorrhages, and hemorrhagic encephalitis,^{1,5,20–24} there is an urgent need to identify the mechanisms that may mediate this increased risk of cerebrovascular events.^{4,5,25} A key discriminating

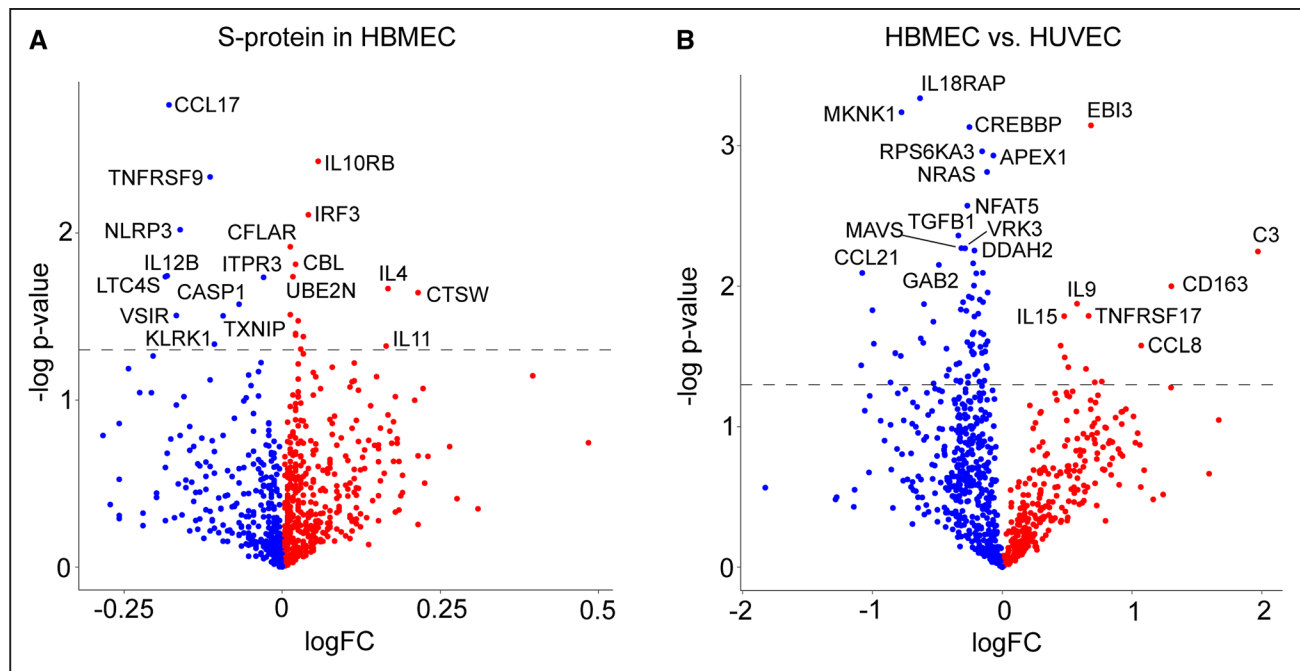


Figure 4. Brain endothelial-specific differential gene expression triggered by recombinant severe acute respiratory syndrome coronavirus-2 (SARS-CoV-2) spike protein exposure.

Normalized differential gene expression measured by direct RNA hybridization after 24-h exposure of human brain microvascular endothelial cells (HBMECs) to 5 μ g/mL SARS-CoV-2 spike protein trimer (S protein; **A**). Differential gene expression in HBMEC after S-protein exposure normalized to expression levels in human umbilical vein endothelial cells (HUVECs; **B**). Dashed line represents $-\log$ adjusted P . LogFC indicates log fold change.

factor in these distinct pathologies are differences in arterial pulsatile or venous steady flow in the brain that may play critical roles in driving viral susceptibility. Thus, because ACE2 levels are relatively low in the brain, we hypothesized that viral susceptibility in the brain may be dependent on additional factors such as fluid shear stress that are difficult to equilibrate with human physiology in monolayer cell culture and even in animal models. Furthermore, we anticipated that brain endothelia may harbor a distinct response to SARS-CoV-2 infection that may be useful in determining individual risk for cerebrovascular complications.

Similar to other coronaviruses, SARS-CoV-2 appears to use the hACE2 protein to gain entry to cells.⁷ In the lung, this viral internalization process also requires the enzymatic activity of TMPRSS2 to cleave the viral spike protein enabling viral entry.⁷ Using human postmortem tissue expression and antibody binding, a single previous study has suggested that ACE2 is expressed in human endothelial cells including those in brain¹¹; however, this study lacked specific images demonstrating ACE2 expression in the brain nor did it specify the vessel size or pattern of ACE2 expression. Gene expression databases from mouse and human provide conflicting data on ACE2 expression but do suggest vascular or perivascular cell expression of ACE2, making the brain endothelia a likely target of circulating virus. In contrast, no data exist on TMPRSS2 expression in vascular endothelium.

Variable expression of ACE2 in cerebrovascular endothelia may be one key factor driving the association of SARS-CoV-2 infection and stroke. Here, we show that in magnetic-activated cell sorting isolated endothelial cells from normal human brain, moderate depth RNA sequencing did not identify robust gene expression of *ACE2* or *TMPRSS2*. Alternative viral cofactors including furin appear enriched in brain endothelia. Using qPCR from cultured brain endothelial cells, *ACE2* mRNA was detectable, though at low levels, and *TMPRSS2* was not detected. At the protein level, ACE2 is detectable in cultured brain endothelial cells while TMPRSS2 is absent. Together, these findings suggest that the basal gene expression of ACE2 in the human brain vasculature is low and that alternative mechanisms for viral coentry to those utilized by SARS-CoV-2 in the lung must be present in the brain.

Critically, using a 3D-printed vessel replica system, we demonstrate that ACE2 gene expression is regulated by fluid shear stress in both undifferentiated endothelial cells and brain microvascular endothelia. A recent report observed that pulsatile shear stress in vascular endothelial cells promotes ACE2 expression and can reduce vascular inflammatory pathways.²⁷ The present findings are consistent with this prior observation and demonstrate that this response is conserved in brain endothelia. In animal models of systemic atherosclerosis, overexpression of ACE2 is associated with a reduction

Table. Key Upregulated Genes Triggered by SARS-CoV-2 S-Protein Binding in Brain Endothelial Cells

Gene	Signaling	Association with SARS-CoV-2
<i>C3</i>	Complement system; myeloid activation	C3 knockout mice had better prognosis and less inflammation in SARS-CoV-1 ¹⁶
<i>CD163</i>	Myeloid inflammation	<i>HLA-DR^{hi} CD163^{hi}</i> monocytes (cluster 2) were present mainly early in severe COVID-19 disease ¹⁷
<i>CCL8</i>	Chemokine signaling; mononuclear cell migration	CCL8 levels increased after viral infection in ferrets infected with SARS-CoV-2 and persisted even after viral load decreased ¹⁵
<i>APOBEC3G</i>	RNA sensing	APOBECs may be involved in viral genome editing (cytosine→uracil hypermutations in virus RNA) ¹⁸
<i>ITGAL</i>	Lymphocyte trafficking; myeloid activation; NK activity	Unknown
<i>EBI3</i>	Other interleukin signaling (IL-27)	Upregulated during acute encephalomyelitis caused by mouse hepatitis virus and inflammation and promotes viral clearance ¹⁹
<i>TNFRSF17</i>	NF-κB signaling	Unknown
<i>OSM</i>	IL-6 signaling; JAK-STAT signaling	Unknown
<i>IL9</i>	IL-2 signaling; JAK-STAT signaling; TH9 differentiation	Unknown
<i>CXCL8</i>	Chemokine signaling; myeloid activation; NF-κB signaling; NLR signaling; RNA sensing; tissue stress; TLR signaling	Significant increase in circulating serum levels of CXCL8 in patients with COVID-19 ¹⁵
<i>IL15</i>	IL-2 signaling; JAK-STAT signaling; myeloid activation; TNF signaling	Clinical trial studying the effects of IL-15 superagonists in removing SARS-CoV-2 virus particles and infected cells (NCT04324996)
<i>CCL24</i>	Chemokine signaling; mononuclear cell migration; NF-κB signaling	Unknown

APOBECs indicates apolipoprotein B mRNA editing enzyme, catalytic polypeptide-like; CCL8, chemokine ligand 8; COVID-19, coronavirus disease 2019; CXCL8, chemokine (C-X-C motif) ligand 8; IL, interleukin; JAK-STAT, janus kinase-signal transducer and activator of transcription proteins; NF-κB, nuclear factor-kappa B; NK, natural killer; NLR, nucleotide-binding oligomerization domain-like receptor; SARS-CoV-2, severe acute respiratory syndrome coronavirus-2; TH9, T helper type 9; TLR, toll-like receptor; and TNF, tumor necrosis factor.

in atherogenic processes and a reduction in the progression of atherosclerotic plaque thickness.^{28,29} In part, this may be due to the local metabolism of angiotensin-II by ACE2 generating angiotensin-1,7 which exerts action on the Mas receptor to inhibit NF-κB (nuclear factor-kappa B) inflammatory cascades.³⁰ Our findings of pulsatile shear stress triggering an increase in ACE2 expression by brain endothelia suggest that local increases in ACE2 levels as a result of high blood pressure or intracranial atherosclerosis may increase the susceptibility to SARS-CoV-2 infection of brain endothelia.

Direct viral infection of the endothelium has been reported in multiple organs in SARS-CoV-2–infected patients,³¹ but data are lacking to support direct viral invasion in the cerebral endothelium. Using the 3D-printed vessel replica model, we demonstrated that S protein–containing liposomes designed to be approximately the size of viral particles (100 nm) and demonstrated to bind to ACE2 can interact with brain endothelia during pulsatile flow. This interaction was not present in monolayer endothelial cells for either HUVECs or HBMECs despite low but detectable levels of ACE2. This suggests that viral-endothelial interactions are at least partially regulated by the dynamic process of blood flow perhaps through a threshold level of ACE2 expression, which we showed is increased in stenotic regions of blood vessels. Using immunocytochemistry, we could not reliably distinguish ACE2 levels between liposome-positive cells

as opposed to those without liposome binding; however, this deserves additional study. While not precisely comparable to in vivo viral-cell interactions, because this ex vivo model uses patient-derived imaging sequences to replicate vessel segments, it is a useful tool to determine what variant cerebrovascular anatomies (stenosis, aneurysms, etc) can increase or decrease viral-endothelial interactions and can provide a moderate throughput platform for therapeutic testing. In addition, we anticipate being able to use this system to determine the enzymatic cofactors needed for viral entry that appear unique in brain endothelia in contrast with other organs.

After establishing the flow dependency of S-protein binding to brain endothelia, we sought to identify the differential response of brain endothelia to SARS-CoV-2 infection. Viral infection with SARS-CoV-2 has been associated with a marked cytokine surge that can potentially increase local and distant thrombotic events.³² Here, we show that simple engagement of ACE2 by recombinant S protein can regulate distinct gene expression patterns in brain endothelia. While this study prespecified a number of immune regulatory genes, S-protein exposure triggers upregulation of a number of genes already implicated in SARS-CoV-2 infection including IL-4 and IL-10 signaling.^{33–35} S-protein binding also appears to downregulate several important pathways in brain endothelia including the inflammasome and apoptotic pathways, potentially facilitating infected cell survival and viral replication. Identification of a brain

endothelia-specific gene expression profile in response to SARS-CoV-2 S-protein exposure is critical to understanding the response of the cerebral vasculature to viral infection. This brain endothelial-specific profile includes several important upregulated pathways. Notably, the most significant upregulated gene by HBMECs compared with HUVECs is C3. The C3 factor plays a central role in the complement cascade, involved in both alternative and classical pathways. When C3 is cleaved into C3a and C3b, the C3a moiety serves as a potent cytokine amplifying the inflammatory signaling, while the binding of C3b to cellular surfaces in combination with other complement factors can lead to cellular destruction. This signal for complement activation already has direct relevance to stroke with C3-null mice demonstrating reduced neuroinflammation in response to infection,³⁶ infarct volumes,³⁷ poststroke inflammation,³⁸ and human subject evidence for plasma exosomes enriched with C3b as a biomarker of cerebrovascular disease.³⁹ IL-27 is induced after intracerebral hemorrhage and hones neutrophil signaling to promote brain repair.⁴⁰ Upregulation of *EBI3*—a component of functional IL-27—suggests this neuroprotective signaling cascade is activated by S-protein binding. Circulating levels of CCL8 are increased in the ferret model of SARS-CoV-2 infection and persist after the viral infection resolves.¹⁵ IL-15 is an immunoregulatory cytokine with strong antiviral properties,⁴¹ for which anti-IL-15 superagonists are currently in clinical trial in SARS-CoV-2-infected individuals (NCT04324996). That viral S protein alone can trigger a brain endothelial-specific response is significant in that it implies unique properties of the S protein:ACE2 interaction that go beyond activation of the renin-angiotensin system. Second, because many of these differentially regulated genes are likely secreted by brain endothelial cells, it may allow for identification of SARS-CoV-2-infected individuals at risk for cerebrovascular complications through serum/plasma monitoring.

Overall, a small number of genes were differentially regulated in response to S-protein exposure. This may be a result of a relatively short incubation period, the use of a targeted gene expression array, and the relatively low basal expression of ACE2 in monolayer HBMECs. Despite this, gene expression differences were detectable and generally fit with the current understanding of how brain endothelial cells respond to other viral infections. Presumably, cellular infection by encapsulated SARS-CoV-2 virus in the presence of shear stress would trigger a more robust gene expression profile that may further identify brain-specific pathways activated by SARS-CoV-2 that can inform our understanding of the cerebrovascular tropism and response to this novel and unique virus.

This study has several important limitations. First, binding of S-protein liposomes to the vessel wall in our 3D model could be driven by mechanisms other than S protein:ACE2 interactions. While this is the primary molecular mechanism for cellular entry of SARS-CoV-2, other

mechanisms may mediate cellular binding under shear stress. Though the S-protein liposomes we generated for this study have high affinity for ACE2 by ELISA, we did not definitively demonstrate that S-protein liposomes require ACE2 for binding in the 3D MCA model, as might be demonstrated by ACE2 knockdown or blocking. Proposed alternative mechanisms including basigin/CD147 have not been convincingly shown to mediate viral:cell interactions.⁴² Despite this, other molecular mechanisms may mediate the interaction between SARS-CoV-2 and brain endothelia. This could be clarified by specific S-protein binding experiments targeting the brain endothelia. Second, ACE2 expression is increased by culturing in 3D using fibronectin as a binding agent even in the absence of flow. While we used monolayer endothelial cultures for comparison in many of these studies, realistic vessel modeling comparing flow versus no flow paradigms may create a more biologically meaningful system for the study of SARS-CoV-2:ACE2 interactions in endothelial cells. Nonetheless, our work highlights the need to appropriately model the organ-specific complications of SARS-CoV-2 infection. In the context of stroke, the effects of blood flow on brain endothelia are significant and functionally alter biologic properties including the susceptibility to SARS-CoV-2 infection. Recognizing this along with the known unique biologic properties of brain endothelia compared with endothelia in other organs, we were able to identify a distinct gene expression profile in brain endothelia that may be useful in determining individualized risk for stroke and other cerebrovascular complications increasingly common during the SARS-CoV-2 pandemic.

CONCLUSIONS

The SARS-CoV-2 cellular receptor ACE2 is poorly expressed by human brain endothelia but can be triggered in a flow-dependent manner. Because of flow-dependent ACE2 expression, cerebral vessels are susceptible to SARS-CoV-2 infection and bind viral S protein under shear stress but likely require unique cofactors for viral entry. Binding of viral S protein triggers a unique gene expression profile in brain endothelia.

ARTICLE INFORMATION

Received September 21, 2020; final revision received October 19, 2020; accepted October 19, 2020.

Presented in part at the American Heart Association Scientific Sessions, November 13, 2020.

Affiliations

Department of Radiological Sciences, David Geffen School of Medicine (N.K., L.G.), Department of Medicine, David Geffen School of Medicine (S.S., T.H.), Department of Neurology, David Geffen School of Medicine (Y.K., J.A., D.S.L., J.D.H.), and Intellectual and Developmental Disabilities Research Center, Semel Institute of Neuroscience (S.D.M., H.I.K.), University of California, Los Angeles. School of Medicine, University of California, San Diego (V.K.). Memory and Aging Center,

University of California, San Francisco (F.E.) and the Veterans Healthcare Administration (J.D.H.) and I01 BX004356 (T.H.).

Acknowledgments

We are indebted to the UCLA COVID-19 Basic, Translational, and Clinical Science Team for intellectual stimulation.

Sources of Funding

This project was supported by a Rapid COVID-19 Response Grant from the American Heart Association No. 20203858 (Drs Kaneko, Hsiai, and Hinman), the University of California Los Angeles W.M. Keck Foundation COVID-19 Research Award Program (Drs Kaneko and Hinman), the Dr Miriam and Sheldon G. Adelson Medical Research Foundation (Drs Muthukrishnan and Kornblum), NINDS NS112799 (Drs Kaneko, Liebeskind, and Hinman), NHLBI HL118650 and HL149808 (Drs Satta and Hsiai), and the Veterans Healthcare Administration I01 BX004356 (Drs Hsiai and Hinman).

Disclosures

On behalf of Drs Satta and Hsiai, the UC Regents intends to submit a provisional patent for the generation of liposomes as detailed in the article. Dr Liebeskind receives support for acting as an imaging core laboratory for Cerenovus, Genentech, Medtronic, and Stryker. The other authors report no conflicts.

Supplemental Materials

Expanded Materials and Methods

Figures I–IV

Data Set

REFERENCES

- Varatharaj A, Thomas N, Ellul MA, Davies NWS, Pollak TA, Tenorio EL, Sultan M, Easton A, Breen G, Zandi M, et al; CoroNerve Study Group. Neurological and neuropsychiatric complications of COVID-19 in 153 patients: a UK-wide surveillance study. *Lancet Psychiatry*. 2020;7:875–882. doi: 10.1016/S2215-0366(20)30287-X
- Tian J, Yuan X, Xiao J, Zhong Q, Yang C, Liu B, Cai Y, Lu Z, Wang J, Wang Y, et al. Clinical characteristics and risk factors associated with COVID-19 disease severity in patients with cancer in Wuhan, China: a multicentre, retrospective, cohort study. *Lancet Oncol*. 2020;21:893–903.
- Zhou F, Yu T, Du R, Fan G, Liu Y, Liu Z, Xiang J, Wang Y, Song B, Gu X, et al. Clinical course and risk factors for mortality of adult inpatients with COVID-19 in Wuhan, China: a retrospective cohort study. *Lancet*. 2020;395:1054–1062. doi: 10.1016/S0140-6736(20)30566-3
- Merkler AE, Parikh NS, Mir S, Gupta A, Kamel H, Lin E, Lantos J, Schenck EJ, Goyal P, Bruce SS, et al. Risk of ischemic stroke in patients with coronavirus disease 2019 (COVID-19) vs patients with influenza [published online July 2, 2020]. *JAMA Neurol*. doi: 10.1001/jamaneurol.2020.2730
- Oxley TJ, Mocco J, Majidi S, Kellner CP, Shoirah H, Singh IP, De Leacy RA, Shigematsu T, Ladner TR, Yaeger KA, et al. Large-vessel stroke as a presenting feature of COVID-19 in the young. *N Engl J Med*. 2020;382:e60. doi: 10.1056/NEJMc2009787
- Teuwen LA, Geldhof V, Pasut A, Carmeliet P. COVID-19: the vasculature unleashed. *Nat Rev Immunol*. 2020;20:389–391.
- Hoffmann M, Kleine-Weber H, Schroeder S, Krüger N, Herrler T, Erichsen S, Schiergens TS, Herrler G, Wu NH, Nitsche A, et al. SARS-CoV-2 Cell entry depends on ACE2 and TMPRSS2 and is blocked by a clinically proven protease inhibitor. *Cell*. 2020;181:271–280.e8. doi: 10.1016/j.cell.2020.02.052
- Qi J, Zhou Y, Hua J, Zhang L, Bian J, Liu B, Zhao Z, Jin S. The scRNA-seq expression profiling of the receptor ACE2 and the cellular protease TMPRSS2 reveals human organs susceptible to COVID-19 infection. *bioRxiv*. Preprint posted online April 18, 2020. doi: 10.1101/2020.04.16.045690
- He L, Mäe MA, Sun Y, Muhl L, Nahar K, Liébanas EV, Fagerlund MJ, Oldner A, Liu J, Genové G, et al. Pericyte-specific vascular expression of SARS-CoV-2 receptor ACE2 – implications for microvascular inflammation and hypercoagulopathy in COVID-19 patients. *bioRxiv*. Preprint posted online May 12, 2020. doi: 10.1101/2020.05.11.088500
- Zhang Y, Chen K, Sloan SA, Bennett ML, Scholze AR, O'Keeffe S, Phatnani HP, Guarnieri P, Caneda C, Ruderisch N, et al. An RNA-sequencing transcriptome and splicing database of glia, neurons, and vascular cells of the cerebral cortex. *J Neurosci*. 2014;34:11929–11947. doi: 10.1523/JNEUROSCI.1860-14.2014
- Hamming I, Timens W, Bulthuis ML, Lely AT, Navis G, van Goor H. Tissue distribution of ACE2 protein, the functional receptor for SARS coronavirus. A first step in understanding SARS pathogenesis. *J Pathol*. 2004;203:631–637. doi: 10.1002/path.1570
- Kaneko N, Mashiko T, Ohnishi T, Ohta M, Namba K, Watanabe E, Kawai K. Manufacture of patient-specific vascular replicas for endovascular simulation using fast, low-cost method. *Sci Rep*. 2016;6:39168. doi: 10.1038/srep39168
- Kaneko N, Mashiko T, Namba K, Tateshima S, Watanabe E, Kawai K. A patient-specific intracranial aneurysm model with endothelial lining: a novel in vitro approach to bridge the gap between biology and flow dynamics. *J Neurointerv Surg*. 2018;10:306–309. doi: 10.1136/neurintsurg-2017-013087
- Khan S, Taverna F, Rohlenova K, Treps L, Geldhof V, de Rooij L, Sokol L, Pircher A, Conradi LC, Kalucka J, et al. EndoDB: a database of endothelial cell transcriptomics data. *Nucleic Acids Res*. 2019;47(D1):D736–D744. doi: 10.1093/nar/gky997
- Blanco-Melo D, Nilsson-Payant BE, Liu WC, Uhl S, Hoagland D, Möller R, Jordan TX, Oishi K, Panis M, Sachs D, et al. Imbalanced host response to SARS-CoV-2 drives development of COVID-19. *Cell*. 2020;181:1036–1045.e9. doi: 10.1016/j.cell.2020.04.026
- Gralinski LE, Sheahan TP, Morrison TE, Menachery VD, Jensen K, Leist SR, Whitmore A, Heise MT, Baric RS. Complement activation contributes to severe acute respiratory syndrome coronavirus pathogenesis. *mBio*. 2018;9:e01753–18.
- Schulte-Schrepping J, Reusch N, Paclik D, Baßler K, Schlickeiser S, Zhang B, Krämer B, Krammer T, Brumhard S, Bonaguro L, et al; Deutsche COVID-19 OMICS Initiative (DeCOI). Severe COVID-19 is marked by a dysregulated myeloid cell compartment. *Cell*. 2020;182:1419–1440.e23. doi: 10.1016/j.cell.2020.08.001
- Di Giorgio S, Martignano F, Torcia MG, Mattiuz G, Conticello SG. Evidence for host-dependent RNA editing in the transcriptome of SARS-CoV-2. *Sci Adv*. 2020;6:eabb5813. doi: 10.1126/sciadv.abb5813
- de Aquino MT, Kapil P, Hinton DR, Phares TW, Puntambekar SS, Savarin C, Bergmann CC, Stohman SA. IL-27 limits central nervous system viral clearance by promoting IL-10 and enhances demyelination. *J Immunol*. 2014;193:285–294. doi: 10.4049/jimmunol.1400058
- Ghosh R, Dubey S, Finsterer J, Chatterjee S, Ray BK. SARS-CoV-2-Associated acute hemorrhagic, necrotizing encephalitis (AHNE) presenting with cognitive impairment in a 44-year-old woman without comorbidities: a case report. *Am J Case Rep*. 2020;21:e925641. doi: 10.12659/AJCR.925641
- Morassi M, Bagatto D, Cobelli M, D'Agostini S, Gigli GL, Bnà C, Vogrig A. Stroke in patients with SARS-CoV-2 infection: case series. *J Neurol*. 2020;267:2185–2192. doi: 10.1007/s00415-020-09885-2
- Katal S, Balakrishnan S, Gholamrezaezhad A. Neuroimaging and neurologic findings in COVID-19 and other coronavirus infections: a systematic review in 116 patients [published online June 27, 2020]. *J Neuroradiol*. doi: 10.1016/j.neurad.2020.06.007
- Delamarre L, Gollion C, Grouteau G, Rousset D, Jimena G, Roustan J, Gaussiat F, Aldigé E, Gaffard C, Duplantier J, et al; NeurolCU Research Group. COVID-19-associated acute necrotising encephalopathy successfully treated with steroids and polyvalent immunoglobulin with unusual IgG targeting the cerebral fibre network. *J Neurol Neurosurg Psychiatry*. 2020;91:1004–1006. doi: 10.1136/jnnp-2020-323678
- Bridwell R, Long B, Gottlieb M. Neurologic complications of COVID-19. *Am J Emerg Med*. 2020;38:1549.e3–1549.e7. doi: 10.1016/j.ajem.2020.05.024
- Aggarwal G, Lippi G, Michael Henry B. Cerebrovascular disease is associated with an increased disease severity in patients with coronavirus disease 2019 (COVID-19): a pooled analysis of published literature. *Int J Stroke*. 2020;15:385–389.
- Deleted in proof.
- Song J, Hu B, Qu H, Wang L, Huang X, Li M, Zhang M. Upregulation of angiotensin converting enzyme 2 by shear stress reduced inflammation and proliferation in vascular endothelial cells. *Biochem Biophys Res Commun*. 2020;525:812–818. doi: 10.1016/j.bbrc.2020.02.151
- Zhang YH, Hao QQ, Wang XY, Chen X, Wang N, Zhu L, Li SY, Yu QT, Dong B. ACE2 activity was increased in atherosclerotic plaque by losartan: possible relation to anti-atherosclerosis. *J Renin Angiotensin Aldosterone Syst*. 2015;16:292–300. doi: 10.1177/1470320314542829
- Dong B, Zhang C, Feng JB, Zhao YX, Li SY, Yang YP, Dong QL, Deng BP, Zhu L, Yu QT, et al. Overexpression of ACE2 enhances plaque stability in a rabbit model of atherosclerosis. *Arterioscler Thromb Vasc Biol*. 2008;28:1270–1276. doi: 10.1161/ATVBAHA.108.164715
- Ingraham NE, Lotfi-Emran S, Thielen BK, Techar K, Morris RS, Holtan SG, Dudley RA, Tignanelli CJ. Immunomodulation in COVID-19. *Lancet Respir Med*. 2020;8:544–546. doi: 10.1016/S2213-2600(20)30226-5
- Varga Z, Flammer AJ, Steiger P, Haberecker M, Andermatt R, Zinkernagel AS, Mehra MR, Schuepbach RA, Ruschitzka F, Moch H. Endothelial cell

infection and endotheliitis in COVID-19. *Lancet*. 2020;395:1417–1418. doi: 10.1016/S0140-6736(20)30937-5

32. Sun X, Wang T, Cai D, Hu Z, Chen J, Liao H, Zhi L, Wei H, Zhang Z, Qiu Y, et al. Cytokine storm intervention in the early stages of COVID-19 pneumonia. *Cytokine Growth Factor Rev*. 2020;53:38–42.
33. Wen W, Su W, Tang H, Le W, Zhang X, Zheng Y, Liu X, Xie L, Li J, Ye J, et al. Immune cell profiling of COVID-19 patients in the recovery stage by single-cell sequencing. *Cell Discov*. 2020;6:31. doi: 10.1038/s41421-020-0168-9
34. Han H, Ma Q, Li C, Liu R, Zhao L, Wang W, Zhang P, Liu X, Gao G, Liu F, et al. Profiling serum cytokines in COVID-19 patients reveals IL-6 and IL-10 are disease severity predictors. *Emerg Microbes Infect*. 2020;9:1123–1130. doi: 10.1080/22221751.2020.1770129
35. Akbari H, Tabrizi R, Lankarani KB, Aria H, Vakili S, Asadian F, Noroozi S, Keshavarz P, Faramarz S. The role of cytokine profile and lymphocyte subsets in the severity of coronavirus disease 2019 (COVID-19): a systematic review and meta-analysis. *Life Sci*. 2020;258:118167. doi: 10.1016/j.lfs.2020.118167
36. Wu F, Zou Q, Ding X, Shi D, Zhu X, Hu W, Liu L, Zhou H. Complement component C3a plays a critical role in endothelial activation and leukocyte recruitment into the brain. *J Neuroinflammation*. 2016;13:23. doi: 10.1186/s12974-016-0485-y
37. Mocco J, Mack WJ, Ducruet AF, Sosunov SA, Sughrue ME, Hassid BG, Nair MN, Laufer I, Komotar RJ, Claire M, et al. Complement component C3 mediates inflammatory injury following focal cerebral ischemia. *Circ Res*. 2006;99:209–217. doi: 10.1161/01.RES.0000232544.90675.42
38. Yang J, Ahn HN, Chang M, Narasimhan P, Chan PH, Song YS. Complement component 3 inhibition by an antioxidant is neuroprotective after cerebral ischemia and reperfusion in mice. *J Neurochem*. 2013;124:523–535. doi: 10.1111/jnc.12111
39. Elahi FM, Harvey D, Altendahl M, Casaleto KB, Fernandes N, Staffaroni AM, Maillard P, Hinman JD, Miller BL, DeCarli C, et al. Endothelial-derived exosomes demonstrate a link between endothelial innate inflammation and brain dysfunction and injury in aging. *bioRxiv*. Preprint posted online June 21, 2019. doi: 10.1101/670083
40. Zhao X, Ting SM, Liu CH, Sun G, Kruzel M, Roy-O'Reilly M, Aronowski J. Neutrophil polarization by IL-27 as a therapeutic target for intracerebral hemorrhage. *Nat Commun*. 2017;8:602. doi: 10.1038/s41467-017-00770-7
41. Verbist KC, Klonowski KD. Functions of IL-15 in anti-viral immunity: multiplicity and variety. *Cytokine*. 2012;59:467–478. doi: 10.1016/j.cyto.2012.05.020
42. Shilts J, Wright GJ. No evidence for basigin/CD147 as a direct SARS-CoV-2 spike binding receptor. *bioRxiv*. Preprint posted online July 26, 2020. doi: 10.1101/2020.07.25.221036